ELSEVIER

Composites Science and Technology 61 (2001) 855–864

COMPOSITES SCIENCE AND TECHNOLOGY

www.elsevier.com/locate/compscitech

In-situ monitoring of damage in CFRP laminates by means of AC and DC measurements

J.C. Abry [a,b], Y.K. Choi [a], A. Chateauminois [a], B. Dalloz [b], G. Giraud [b], M. Salvia [a,*]

[a] *Laboratoire d'Ingénierie et Fonctionnalisation des Surfaces, UMR CNRS 5621, Ecole Centrale de Lyon, BP 163-69131 Ecully Cedex, France*
[b] *Laboratoire de Physique des Systèmes Désordonnés, UMR CNRS 139, Université de Provence, Marseille, France*

Received 14 February 1999; received in revised form 16 November 1999; accepted 4 July 2000

Abstract

Periodical maintenance NDT-based inspections are generally used for almost all complex technological structures today. The idea of using specific sensors integrated in the structure for structural real time monitoring (or health monitoring) is now in progress. Carbon-fibre-reinforced polymers (CFRP) are increasingly used as structural parts, especially in the aircraft industry. This work deals with the possibility of detecting in-situ damage in CFRP by the use of DC or AC electrical property measurements. Monotonic tests under post-buckling bending conditions are being performed on cross ply $[0/90]_s$ and $[90/0]_s$ carbon/epoxy laminates. The monitoring of electrical resistance and capacitance changes, linked to the modifications of the conduction paths in the composite, and occurrence of voids during loading, allowed the detection of damage growth. It seems that DC electrical conduction allows to detect fibre failure, but AC measurements are more suitable for monitoring matrix cracks (delamination, fibre/matrix debonding or transverse cracks).

Keywords: Health monitoring; Carbon-fibre-reinforced polymers; Composite materials; Electrical resistance; Capacitance

1. Introduction

The classical methods for periodical maintenance use many NDE techniques which require extensive human involvement and expensive procedures. Moreover, this kind of periodical inspection cannot give any information concerning accidents and failures occurring between two successive overhauls. In order to overcome such shortcomings it is now possible to use 'sensitive' material. A material or a structure is said to be 'sensitive' when it includes sensors providing real-time information about the material itself, or its environment. Continuous health monitoring of materials would result in improved durability and safety of structures. On-line health monitoring sensors must meet three requirements. They must be small in size (with no damage to the structure), offer the possibility of being located in remote and inaccessible areas of the structure, and they must be able to transmit information to a central processor. This information must be in direct relation with the physical process being monitored and the properties and performances that is to be maintained. Evidently they must compete in sensitivity with conventional NDE techniques and be able to monitor a sufficient area of the structure.

One way, which could be the most natural, to obtain a 'sensitive' material is to use the material itself or a part of this material-system as sensor. Evidently this is possible in the case of carbon-fibre-reinforced polymers (CFRP) or hybrid glass/carbon FRP [1,2], since carbon fibres are electrical conductors ($\rho \sim 1.5 \times 10^{-5}\Omega$ m) embedded in an insulating matrix ($\rho \sim 10^{13}-10^{15}\Omega$ m). A transverse conduction also exists by contacts between neighbouring fibres and plies. Indeed, carbon fibres are not perfectly aligned in the composite and the electrical conduction occurs not only in the direction of the fibres, but also in the transverse directions for unidirectional as well as for multidirectional laminates. The measurement of the global electrical resistance appears to be a valuable technique that can be used to monitor the fibre fracture and the delamination process connected with a modification of the resistive tracks in the laminates [3–6]. Dielectric analysis [7] is currently available, or in progress, for cure monitoring of thermoset resins. For

* Corresponding author. Tel.: +33-4-7218-6431; fax: +33-4-7833-1140.
E-mail address: michelle.salvia@ec-lyon.fr (M. Salvia).

0266-3538/01/$ - see front matter
PII: S0266-3538(00)00181-0

the same way, Schulte and Wittich [8] have shown that the measurement of the complex impedance of CFRP cross-ply during tensile loading is also available for damage detection, such as fibre failure or matrix cracking.

In many composite applications the final design involved significant flexural loading. Cross-ply laminates underwent complex damage processes involving transverse cracks, debonding of the fibre-matrix, delamination and fibre failure. Moreover, the damage mechanisms of such composites subjected to flexural loading depend on the stacking sequence, that is of the external ply type (0° or 90°). In this study, DC and AC electrical measurements were used to detect accurately the threshold of the damage process in cross-ply laminates and to monitor the damage growth.

2. Materials and experimental methods

2.1. Materials

Composites used in this study were carbon fibre/epoxy laminates made from epoxy matrix (CIBA 913) and TOHO high resistance fibres (HTA7). Manufacture was achieved by prepreg and epoxy resin lay-up with subsequent curing in the autoclave (1.5 h at $T=125$°C and $P=7$ bars). As the failure behaviour of cross-ply laminates under bending loading depended very much on the stacking arrangement, two stacking sequences were considered, namely $[90/0]_s$, $[0/90]_s$. The volume fraction of carbon fibres is 0.50 (16 prepreg layers and eight epoxy resin layers, each resin being placed between each two prepreg layers) and the thickness is about 2.2 mm. Fig. 1 shows a microscopic view of polished sample section after curing for the two stacking sequence. The average ply thickness is about equal to 140 μm.

The temperature T_α of the thermomechanical transition associated with the glass transition was 125°C, as measured by torsional dynamical spectrometry, at a frequency of 1 Hz and a scan rate of 2°C/min.

2.2. Experimental methods

The samples (100 mm long, 10 mm wide, 2.2 mm thick) were subjected to monotonic post-buckling bending tests described elsewhere [5,9] with a constant cross-head rate of 2 mm/min. The tests consisted of applying an axial compressive load to the sample. The specimen is gripped at each end, and can accommodate the local deformation by in plane rotation. When the applied load, P, reaches the Euler critical load, the specimen's buckling induces a flexural moment (Figure 2). The flexural mean stress at failure was 1190±12 MPa and 928±62 MPa for the [0/90] and [90/0] laminates respectively. The elongation to break was 2.05%±0.3% and 2.25%±0.3% for the [0/90] and [90/0] laminates respectively. A HP3485A multimeter was used to take DC electrical measurements in longitudinal direction. A constant intensity of 10 mA was delivered by a generator. The copper electrodes (10 mm×10 mm×0.1 mm) were deposited on the fibres, after polishing to suppress the insulating matrix surface layer, by electrolytic deposition [5]. They were located on the tensile side at the ends of the specimen as shown in Fig. 2a, because the damage occurrence on this side at the beginning.

AC measurements were carried out in the direction perpendicular to the fibre layers. The electrodes (copper film of about 20 μm) are soldered on opposite sides with an epoxy resin and are located close to the maximal strain zone, i.e. the middle of the sample (Fig. 2b). The complex impedance (Z' and Z'') of the specimen between the electrode was measured by a Solartron (SI 1260) impedancemeter (frequency = 100 kHz and voltage = 500 mV). As mentioned previously, CFRPs can be considered as electric conducting materials (fibres) and an insulator (matrix) assembly. According to this assumption, CFRP laminates can be said to behave like an RC circuit [8] such that:

$$R=\frac{Z'^2+Z''^2}{Z'} \tag{1}$$

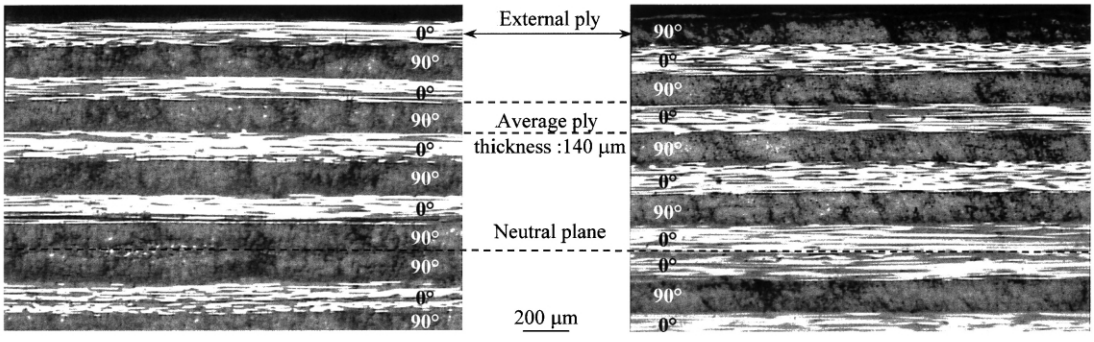

Fig. 1. Polished section of (a) [0/90] laminate and (b) [90/0] laminate.

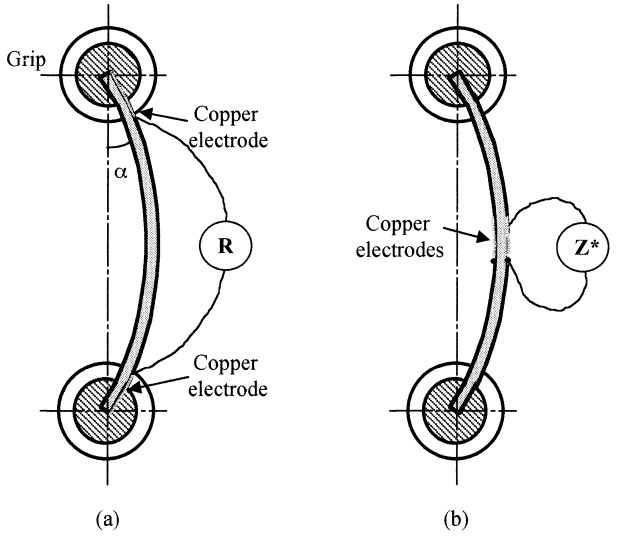

Fig. 2. Schematic illustration of the post-buckling bending test: electrode location used for (a) DC and (b) AC measurements.

$$C = \frac{-Z''}{(Z'^2 + Z''^2)\omega} \tag{2}$$

The load P and the electrical resistance R, or impedance versus the longitudinal displacement δ was plotted. P and δ values were then used to compute the maximum stress and strain on the tensile side of the sample.

3. DC measurements

3.1. [0/90] laminates

The [0/90] cross-ply composites showed linear mechanical behaviour up to the appearance of macroscopic damage occurring at strain 2.14% (Fig. 3). At the same time, there was at the beginning of testing a progressive, but slight linear increase in resistance (ΔR) until $\varepsilon = 0.9\%$ where a deviation from linearity was observed. Finally, in most of the cases the sample failed suddenly on the tensile side, by failure of the first plies without any previous individual fibres or fibre bundles breakages in most of the cases. This led to a large rise in electrical resistance associated with a drop in stress.

In order to use such resistance measurements for sensing purposes, i.e. long before macroscopic damage, it is necessary to study precisely the phenomena (initiation and growth of the micro-damages) occurring in the reversible part of the stress/strain curve. Therefore, successive loading-unloading cycles were performed at an increasing strain within 20% of the ultimate stress to failure range. After each cycle, microscopic observations were carried out on sample edges polished by metallographic methods before the test. These optical observations on edges of the [0/90] laminates near the central zone of the sample, after each cycle, showed that the damage was first initiated in the external longitudinal ply by fibre failure. First failures were clearly observed after the second cycle. Fibre fracture caused high shear

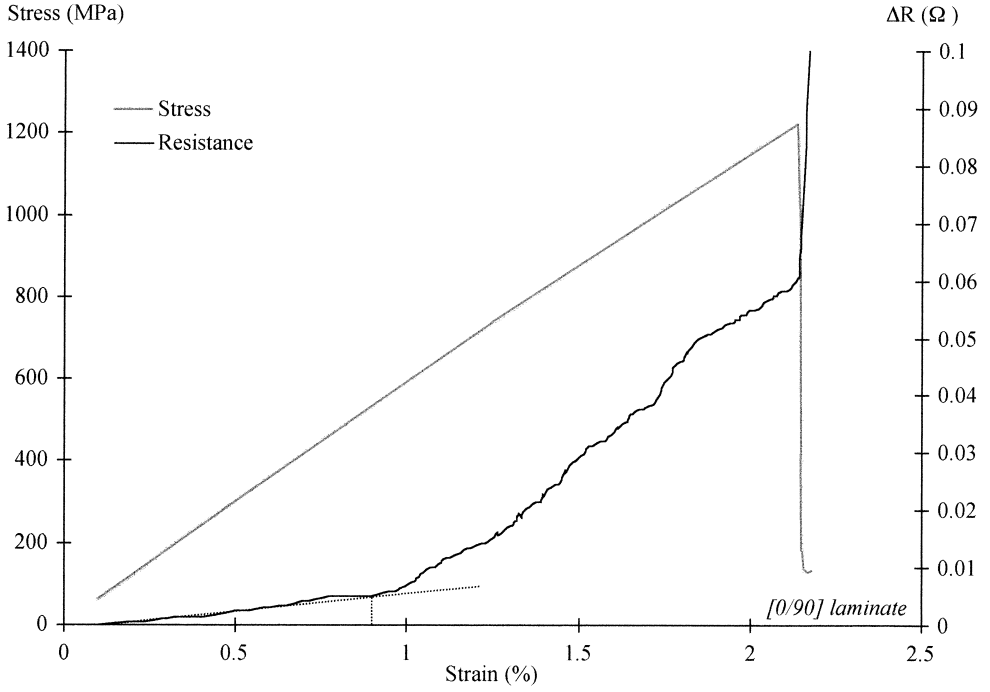

Fig. 3. Changes in stress and electrical resistance as a function of the applied strain during a flexural monotonic loading for [0/90] composite.

stress at the fibre/matrix interface, and longitudinal cracks with fibre/matrix debonding began to appear in the longitudinal ply. Fibre failure and associated fibre/matrix debonding density increased continuously, even in internal plies until failure (Fig. 4). From $\varepsilon = 1.51\%$ (cycle 2) a few normal cracks occur parallel to the fibres in the 90° plies, close to the tensile side, by debonding at fibre/matrix interface (Fig. 5). However cracks will grow across the entire thickness of the transverse ply only at the late stage of the tests, i.e. just before failure. Cracks in different plies (five plies) close to the tensile side were connected through delamination and final failure occurred when the external longitudinal ply supporting the highest applied load failed. The post-mortem microscopic observations (Fig. 6) pointed out that the damage process leading to the final failure was essentially governed by fibre fractures.

Fig. 7 shows the maximal stress and $\Delta R = R - R_0$ (R_0 is the electrical resistance at the beginning of the first cycle) against strain for the different loading/unloading cycles. No significant changes were noted in the macroscopic stiffness during cycles, but both the maximum and minimum resistance for each, increased with successive strain cycles. During the first cycle a very slight increase is observed at the beginning (that is until about a strain of 0.9%). Then the resistance increases faster. During unloading a slight decrease of the resistance occurs then followed by a faster drop. With each progressive further cycle the sample was strained to a slightly greater maximal strain than the preceding one. The new loading curve appeared almost superposed on the unloading one of the previous cycle until the previous maximal strain was reached. Beyond this strain a sharp growth of the electrical resistance was observed.

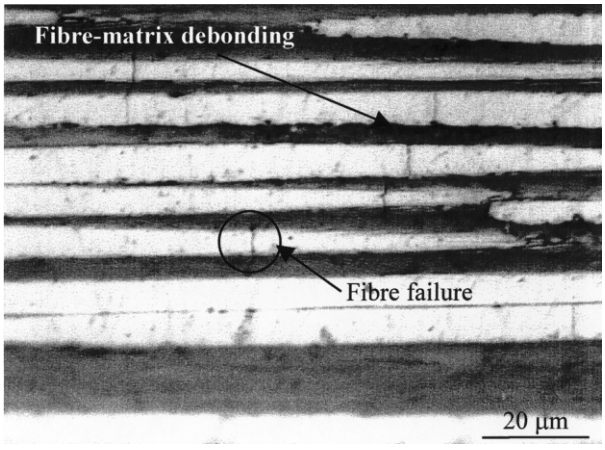

Fig. 4. [0/90] Laminate: fibre failure and fibre/matrix debonding occurring in the external longitudinal ply ($\varepsilon = 1.89\%$).

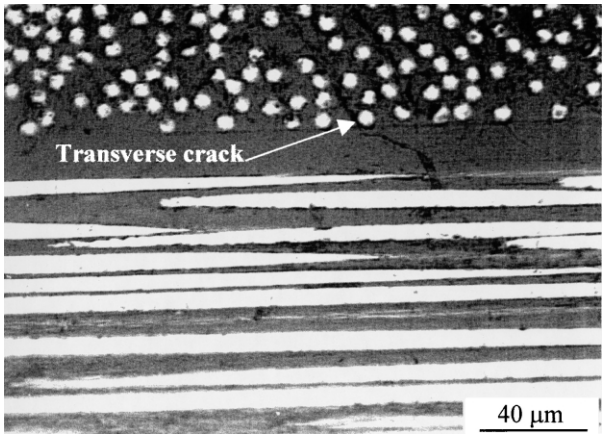

Fig. 5. [0/90] Laminate: normal cracks occurring in matrix-rich region of the transverse ply close to the tensile side ($\varepsilon = 1.89\%$).

In the first cycle, the linear resistance rise according to strain was mainly linked to the elastic elongation of the fibres. It may have also been due though not significantly to the alignment of misaligned fibres by decreasing fibre to fibre contacts in the 0° ply on the tensile side of the sample. Effectively, it was shown previously that for a 0° UD laminates subjected to flexural loading, the linear increase of the resistance at the very beginning of the test was mainly due to the elongation of fibres [5]. This result can be used in this experimental configuration because the conduction occurred mainly in the first 0° ply. This is a consequence of the fact that the quasi-insulator nearest plies (90° and pure resin) prevent the current lines from progressing down the thickness of the sample. For this 0° ply the resistance was given by the following relationship (the resistance of contacts was neglected):

$$R = \frac{\rho_f L}{b h_p v_f} \tag{3}$$

where h_p corresponds to the thickness of the external ply (140 μm measured by microscopic observation), L the sample length, v_f to the fibre-volume fraction (0.5) and

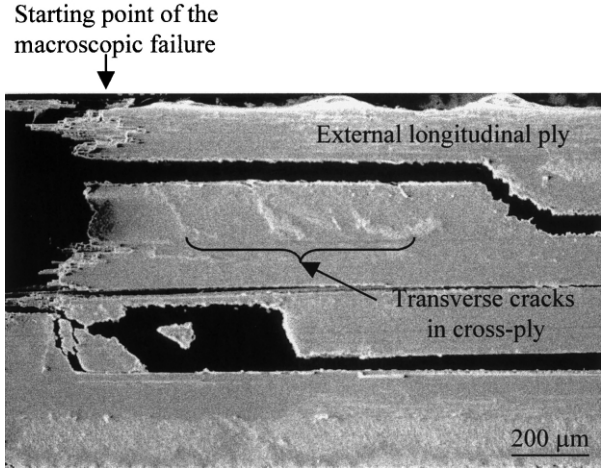

Fig. 6. Post-mortem scanning electron micrograph of a failure feature observed on a [0/90] laminate subjected to four loading/unloading cycles before failure.

ρ_f to the resistivity of the fibre ($1.6 \times 10^{-5}\Omega$ m as given by the manufacturer).

As previously shown [5], the elongation ΔL of the tensile side of the specimen can be described by the following relationship:

$$\Delta L = h\alpha \tag{4}$$

where α is the angular deflection linearly related to the maximal strain (Fig. 2) and h the sample thickness.

The rise in resistance as a result of the increase of length can be described by a linear relationship according to α or ε as observed experimentally at the beginning of the test (at strain below 0.9%) where practically no fibres broke as shown by optical microscopy:

$$\Delta R = \frac{\rho_f}{b h_p v_f} h\alpha \tag{5}$$

Moreover, the average experimental slope (3×10^{-2} Ω rad^{-1}) and the theoretical slope (4×10^{-2} Ω rad^{-1}) were of the same order of magnitude. The acceleration of the resistance rise at strain beyond 0.9% was linked to microscopic damage associated with isolated fibre failures whose density increased gradually with the strain (even if the modulus did not seem weakened). The enhanced decrease in resistance at the end of the unloading phase could be a result of the fact that the ends of previously broken fibres were again in contact, resulting from fibres slipping reversibly in their socks. These contacts disappeared again during the first part of the loading phase of the subsequent cycle. For strains larger than the previous maximal one, new fibre breaks happened involving an increase of resistance. In spite of the fact that the variation of the resistance versus the strain is non-linear, such measurements allow us to monitor the strain. It is interesting to note that the sensitivity is highly precise for the low strains that are in the range of use of the composite parts. Moreover the evolution of the global resistance level can give information about the occurrence of microdamage. It seems possible to define a critical level of resistance increase ΔR as a warning in health monitoring approaches. Similar results were yet shown in the case of UD carbon fibre/glass-fibre-hybrid-reinforced polymers with 0.3–0.4% of carbon fibre volume content [2] and UD carbon epoxy laminates with a fibre-volume fraction of about 40% [5].

3.2. [90/0] laminates

In the case of [90/0] laminates, the stress/strain relation is linear up to $\varepsilon \sim 0.9\%$, beyond which the material showed a slightly smaller slope than the initial tangent slope. ΔR increased gradually with increasing strain, and then increased faster as the strain rose beyond 0.9%. The final failure involving four plies closer to the tensile side, occurred at $\varepsilon = 2.47\%$ leading to an abrupt increase of ΔR associated to the stress drop (Fig. 8).

As in the preceding case ([0/90] laminates), and in order to monitor the beginning of the damage, successive

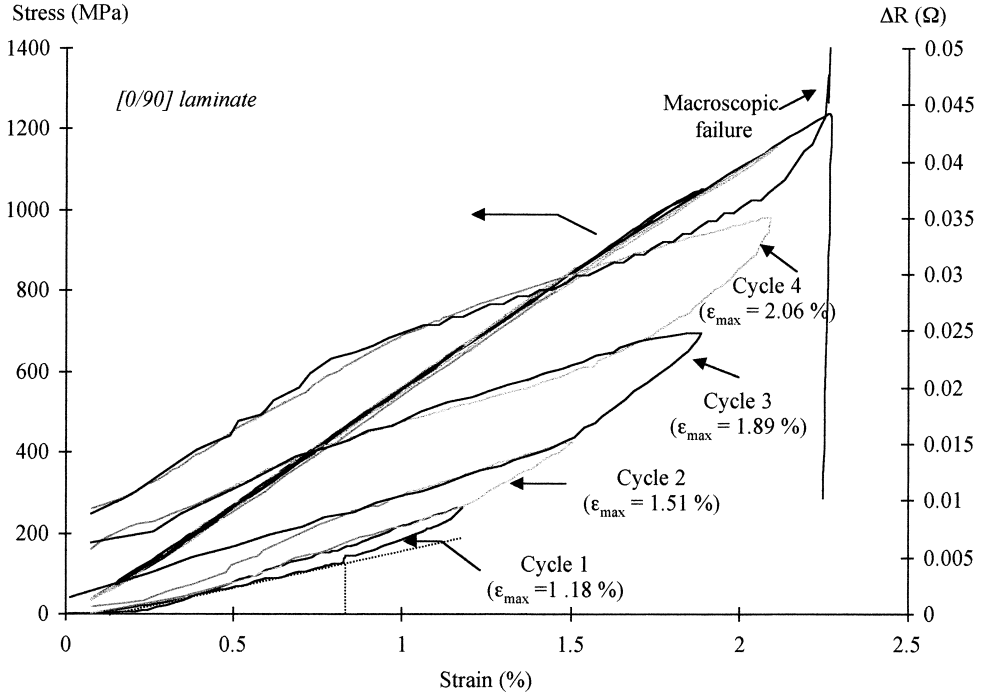

Fig. 7. Changes in stress and electrical resistance as a function of the applied strain during loading/unloading cycles at increased applied maximum strains for [0/90] laminate.

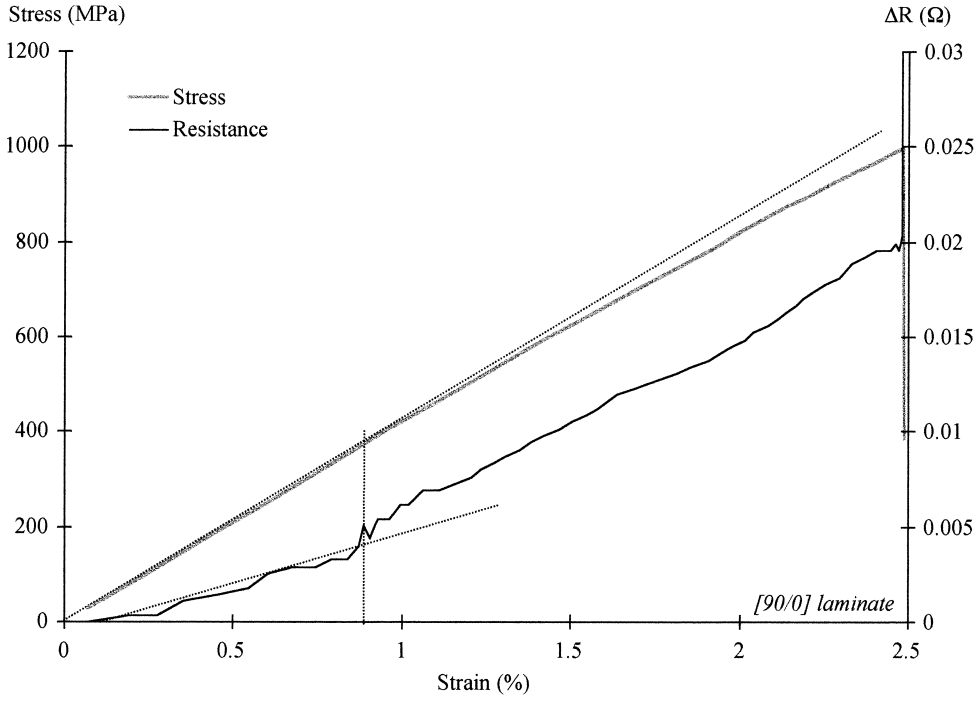

Fig. 8. Changes in stress and electrical resistance as a function of the applied strain during a flexural monotonic loading for [90/0] composite.

loading/unloading cycles were performed at increasing, but low, strains with microscopic observations. For such composites the transverse (90°) external ply failed first at weakest locations (in zones with the higher fibre-volume fraction) by debonding at the fibre-matrix interface. It led to intralaminar cracks perpendicular to the tensile direction propagating through the entire width of the ply. First transverse cracks were observed after the first cycle, i.e. for strain equal to 1.27% (Fig. 9) with the result that the modulus little decreased as observed in Fig. 8. These cracks are unable to extend over the adjacent ply in which the fibres lie in the 0° loading direction. Nevertheless, as the load increased, two modes of damage growth were observed, probably as a result of strong interfaces between adjacent plies: further cracks were formed away from the first ones, and owing to high stress concentrations at crack tips it resulted in fibre failure ahead of the transverse cracks in the first longitudinal 0° ply (Fig. 10). These failures were observed on edge from $\varepsilon = 1.4\%$ and the final failure occurred at $\varepsilon = 2.4\%$ when the longitudinal ply closer to the tensile side carrying the load was sufficiently weakened. It is interesting to note that no delamination was observed even after failure (Fig. 11).

The results obtained using DC measurements were very similar for the two types of laminates even if the

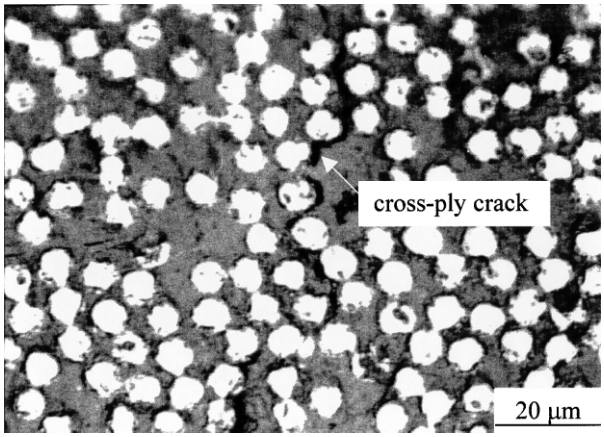

Fig. 9. [90/0] Laminates: cross-ply crack occurring in the external transverse ply ($\varepsilon = 1.4\%$).

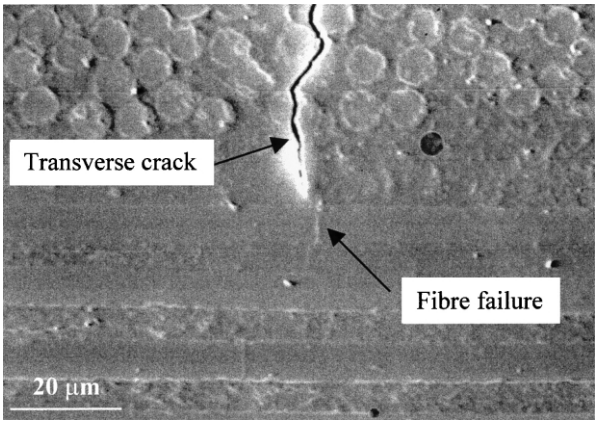

Fig. 10. [90/0] Laminates: fibre failure ahead of a transverse crack (post-mortem view).

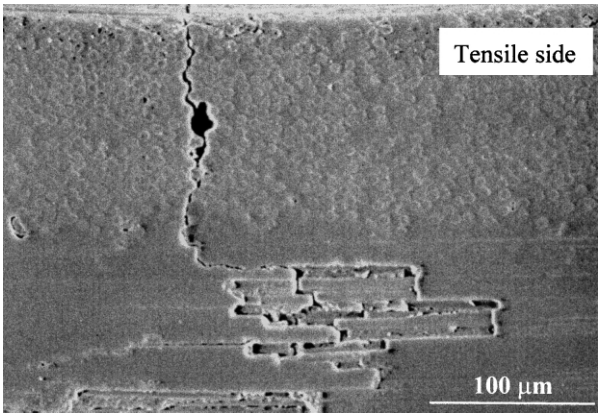

Fig. 11. Post-mortem scanning electron micrograph of a failure feature observed on a [90/0] laminate subjected to three loading/unloading cycles before failure.

values were more scattered in the latter case (Fig. 12). The shape of the cycles can be qualitatively understood with the help of the same hypothesis as for [0/90] laminates, that is: elongation followed by failure of fibres during the loading phase of the cycle and contraction of the reinforcement followed by reversible slip of broken fibres in their socks as a function of the decreasing strain. It can be concluded that only the fibre failure can be clearly detected. So, as for the [0/90] laminates (but not on the same level), it could be possible to postulate a critical threshold giving a warning in health monitoring approaches.

4. AC measurements

Figs. 13 and 14 gave typical relative through-thickness capacitance ($C_{rel} = \Delta C/C_0$) and resistance ($R_{rel} = \Delta R/R_0$) as well as stress according to strain, respectively, for [0/90] and [90/0] laminates loaded up to failure. Whatever the stacking sequence, two regions can be schematically identified. The initial region is characterised by a slow linear increase of resistance and decrease of capacitance with increasing stress. In the following region, the dielectric impedance variation versus strain showed a different shape, depending on laminate construction. The [0/90] laminates exhibited moderate non-linear R_{rel} and C_{rel} strain behaviour with increase of resistance and decrease of capacitance until the final failure, whereas for [90/0] laminates R_{rel} increased and C_{rel} decreased more abruptly as the strain increased.

For each laminate, the onset of non-linearity of the resistance or capacitance/strain curve defined the strain limit between the two regions that is about 0.9% for the two-stacking sequence. These limits indicated the threshold of the cracking process as observed by previous microscopic observations and DC measurements. Moreover, the damage growth process can explain the dependence on the type of laminate of the nature of the resistance and capacitance change with strain in the second region.

Indeed, fibre/matrix debonding led to a decrease of the capacitance of the laminates, linked to the opening

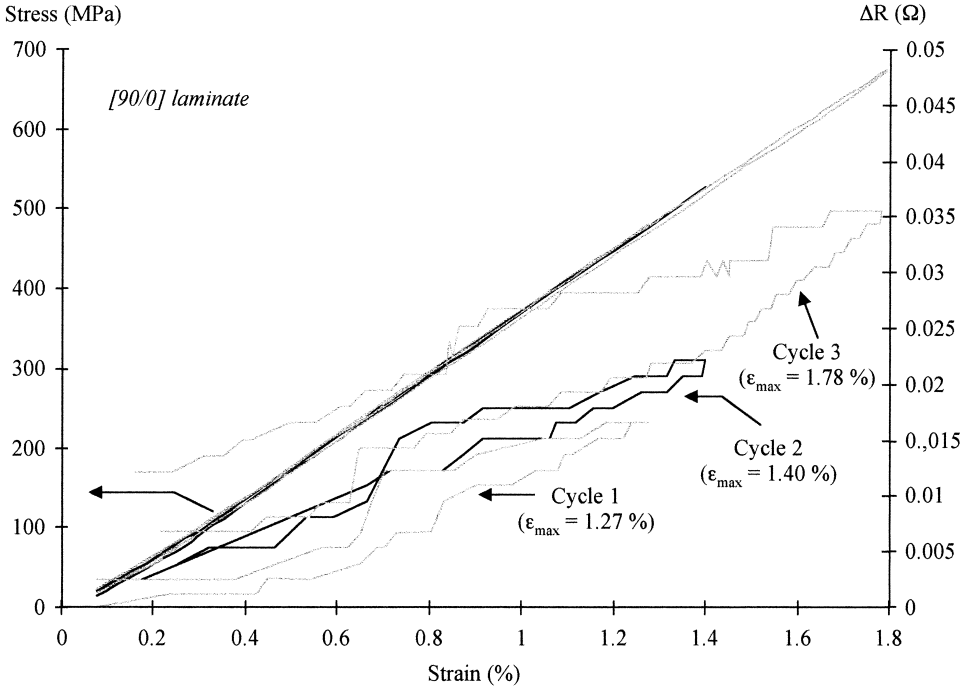

Fig. 12. Changes in stress and electrical resistance as a function of the applied stain during loading/unloading cycles at increased applied maximum strains for [90/0] laminate.

of cracks. As previously mentioned, fibre/matrix debonding occurred in the 90° ply and in longitudinal plies near the tip of the broken fibres. The microscopic observation showed that in the case of [90/0] composites, the crack density in the transverse ply increased abruptly beyond the strain level corresponding to the stress-strain curve 'knee' (~ 0.9%). Then, these cracks led to fibre breaks in the adjacent 0° ply and associated fibre/matrix debonding. These phenomena induced a marked fall of the capacitance with the strain. For [0/90]

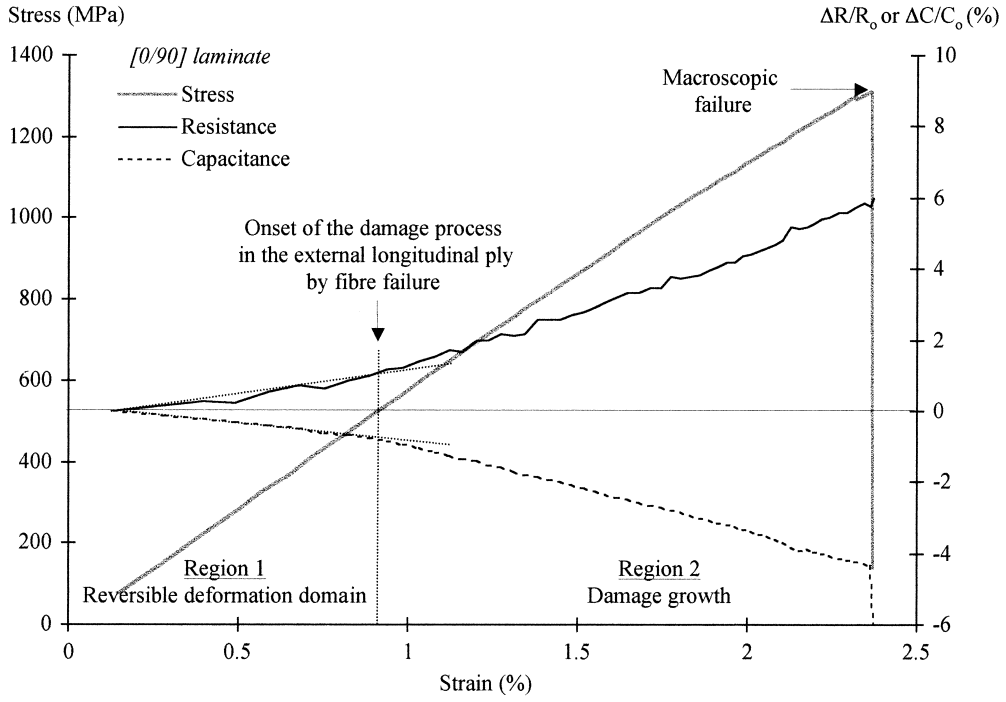

Fig. 13. Changes in stress and AC measurements as a function of the applied strain during a flexural monotonic loading for [0/90] composite.

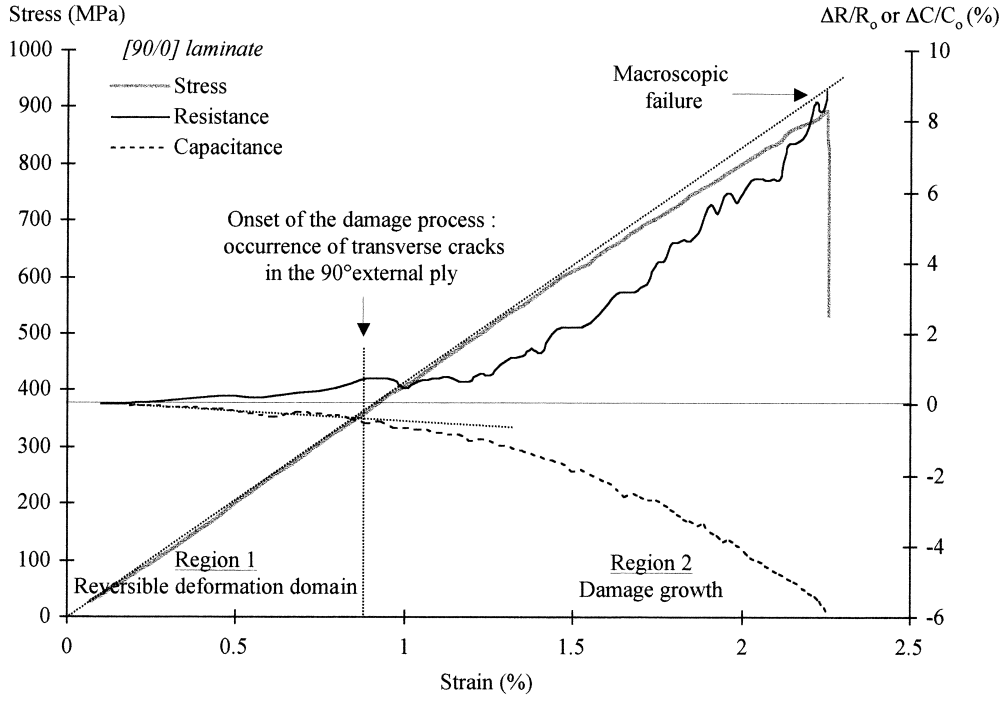

Fig. 14. Changes in stress and AC measurements as a function of the applied strain during a flexural monotonic loading for [90/0] composite.

laminates very few cracks were observed in transverse plies before failure and the continuous decrease of capacitance is mostly a consequence of the fibre/matrix debonding at fibre failure occurring at a strain level of about 0.9%.

The transverse resistance is connected to the number of fibre-to-fibre conduction paths. Therefore, the resistance is highly sensitive to matrix failures with the result that reducing the number of fibre-to-fibre conduction paths induces a reduction of the current flow in the direction perpendicular to the fibres layers. The marked increase in resistance for the [90/0] laminates associated to a flattening of the modulus beyond $\varepsilon \sim 0.9\%$ is a result of the occurrence of off-axis ply failures. For the [0/90] materials the gradual rise of resistance have probably the same origin than the decrease of capacitance.

The resistance and capacitance evolution at the beginning of the test cannot be linked to visible microscopic damage. This weak evolution was probably associated with the modification of the fibre/fibre resistive paths under stress. However, in order to explain the sense of this effect, it is necessary to suppose an asymmetric action of the stresses, the tensile stress having more of an effect than the compressive one. Complementary work is necessary in order to clearly understand this part of the results.

Nevertheless, whilst taking into account all the AC curves, it was concluded that AC measurements provide an effective means to detect damage development in cross-ply laminates, especially matrix cracks, and can be used in the health-monitoring approach.

5. Conclusion

Measurements of the electrical resistance (DC experiments) and AC properties (resistance and capacitance) provide accurate means to monitor the in-situ evolution of damage nucleation and growth in cross-ply CFRP laminates particularly for internal damage. A critical change of resistance or capacitance variation can be defined as a warning for the health monitoring approach during monotonic or cyclic loading. It is important to note the complementary aspects of these two types of measurements: DC technique is mainly sensitive to fibre failures, and AC measurements provide information essentially on the development of matrix cracks (intraply matrix cracks and interply delamination). The combined use of these two methods will enable the detection as well as the qualitative identification of various damage mechanisms.

Moreover, the resistance measurements can be used to monitor the strain in spite of the non-linear relation during monotonic loading of cross-ply CFRP laminates. It is also probably possible to go further: it was shown in a previous paper [10] that a linear relationship was observed between electrical resistance increase and stiffness loss in fatigue conditions for CFRP UD laminates.

This kind of sensor would be employed to monitor in-situ the structural integrity of composite industrial component (primary structures) such as aircraft wings, helicopter blades in real time and possibly low cost compared with current composite structure inspection techniques. In particular, this kind of sensor is compatible with the fabrication of the material from which the structure was made and does not adversely affect the behaviour of the structure being monitored. Nevertheless a large amount of development needs to be done in this area:

- A network of electrodes must be implemented throughout the structure in order to extract the appropriate local information. These electrodes need to be structurally robust with respect to in-service life conditions.
- The system estimates the condition of the structure (loading, structural state) based on data comparison between unloaded and healthy structure reference data and continuous measurements in real time during service. A pre-stored resistance (or/and capacitance) acquisition on the real structure before loading is then required, composite materials being essentially inhomogeneous and of various nature.
- Moreover, there is a need for simultaneous resistance/capacitance and temperature measurements coupled to a reliable thermo-electrical modelling of the monitored material. Without any load or damage the resistivity of such a material varies with temperature. This variation is due, firstly, to the difference between the expansion coefficients of the material components that modify fibre to fibre contacts and, secondly, to the semi-conductor nature of carbon fibre, even if this effect is small in the temperature range of composite structure use.
- Further more, the sensing system must also be compatible with the operating environment (electrical, magnetic environment) that the structure will experience. Experiments have to be performed in this way on real parts.

Acknowledgements

The authors are grateful to the DGA (SREA) for supporting this work and Hexcel Composites (Dagneux, France) for supplying materials and technical assistance. The authors also wish to thank M.F. El Fassi for scanning electron micrography.

References

[1] Schulte K, Baron Ch. Load and failure analyses of cfrp laminates by means of electrical resistivity measurements. Composites Science and Technology 1989;36:63–76.

[2] Muto N, Yanagida H, Nakatsuji T, Sugita M, Ohtsuka Y, Arai Y, Saito C. Intelligent CFGFRP composites with self-diagnostic function for preventing fatal fracture. Sensors and Materials 1994;6(1):45–62.

[3] Thiagarajan C, Sutherland I, Tunnicliffe D, Irving PE. Electrical potential techniques for damage sensing in composite structures. In: Proc. of 2nd Eur. Conf. on Smart Struct. and Mater., 1994. p. 128–31.

[4] Ceysson O, Salvia M, Vincent L. Damage mechanisms characterisation of carbon fibre/epoxy laminates by both electrical resistance measurements and acoustic emission analysis. Scripta Materialia 1996;34(8):1273–80.

[5] Abry JC, Bochard S, Chateauminois A, Salvia M, Giraud G. In situ detection of damage in CFRP laminates by electrical resistance measurements. Composites Science and Technology 1999; 59:925–35.

[6] Wang X, Chung DDL. Sensing damage in carbon fiber polymer–matrix composites during fatigue by electrical measurements. In: SPIE Conference on Sensory Phenomena and Measurement Instrumentation for Smart Structures and Materials, San Diego, CA, 1998. p. 36–47.

[7] Kranbuehl D, Aandahl H, Haralampus N, Newby W, Hood D, Boiteux G, Seytre G, Pascault JP, Maazouz A, Gerard JF, Sautereau H, Chailan JF, Loos AC, MacRae JD. Use of in situ dielectric sensing for intelligent processing and health monitoring. In: Gobin PF, Tatibouet J, editors. Third Int. Conference on Intelligent Materials Lyon, vol. SPIE 2779, 1996. p. 112–117.

[8] Schulte K, Wittich H. The electrical response of strained and/or damaged polymer matrix composites. In: Street K, Poursatip A, editors. 10th Int. Conference on Composite Materials vol. 5, 1995, p. 315–325.

[9] Large-Toumi B, Salvia M, Vincent L. Fiber/matrix interface effect on monotonic and fatigue behavior of unidirectional carbon/epoxy composites. In: Spragg CJ, Drzal LT, editors. Fiber, matrix, and interface properties (ASTM STP 1290). American Society for Testing and Materials, 1996. p. 182–200.

[10] Abry JC, Bochard S, Chateauminois A, Salvia M, Giraud G. In situ monitoring of flexural fatigue damage in CFRP laminates by electrical resistance measurements. In: Tomlinson GR, Bullough WA, editors. Smart Materials and Structures, 4th ESSM and 2nd MIMR Conference, Harrogate, 1998. p. 389–396.